Energy level alignment and quantum conductance of functionalized metal-molecule junctions

Density functional theory versus GW calculations

Jin, Chengjun; Strange, Mikkel; Markussen, Troels; Solomon, Gemma C.; Thygesen, Kristian Sommer

Published in:
Journal of Chemical Physics

Link to article, DOI:
10.1063/1.4829520

Publication date:
2013

Document Version
Publisher's PDF, also known as Version of record

Energy level alignment and quantum conductance of functionalized metal-molecule junctions: Density functional theory versus GW calculations

Chengjun Jin, Mikkel Strange, Troels Markussen, Gemma C. Solomon, and Kristian S. Thygesen

Citation: The Journal of Chemical Physics **139**, 184307 (2013); doi: 10.1063/1.4829520
View online: http://dx.doi.org/10.1063/1.4829520
View Table of Contents: http://scitation.aip.org/content/aip/journal/jcp/139/18?ver=pdfcov
Published by the AIP Publishing

Energy level alignment and quantum conductance of functionalized metal-molecule junctions: Density functional theory versus GW calculations

Chengjun Jin,[1] Mikkel Strange,[2] Troels Markussen,[1] Gemma C. Solomon,[2] and Kristian S. Thygesen[1,a)]
[1]*Center for Atomic-scale Materials Design, Department of Physics, Technical University of Denmark, DK-2800 Kgs. Lyngby, Denmark*
[2]*Nano-Science Center and Department of Chemistry, University of Copenhagen, Universitetsparken 5, 2100 Copenhagen Ø, Denmark*

(Received 14 June 2013; accepted 28 October 2013; published online 11 November 2013)

We study the effect of functional groups (CH_3*4, OCH_3, CH_3, Cl, CN, F*4) on the electronic transport properties of 1,4-benzenediamine molecular junctions using the non-equilibrium Green function method. Exchange and correlation effects are included at various levels of theory, namely density functional theory (DFT), energy level-corrected DFT (DFT+Σ), Hartree-Fock and the many-body GW approximation. All methods reproduce the expected trends for the energy of the frontier orbitals according to the electron donating or withdrawing character of the substituent group. However, only the GW method predicts the correct ordering of the conductance amongst the molecules. The absolute GW (DFT) conductance is within a factor of two (three) of the experimental values. Correcting the DFT orbital energies by a simple physically motivated scissors operator, Σ, can bring the DFT conductances close to experiments, but does not improve on the relative ordering. We ascribe this to a too strong pinning of the molecular energy levels to the metal Fermi level by DFT which suppresses the variation in orbital energy with functional group. © *2013 AIP Publishing LLC*. [http://dx.doi.org/10.1063/1.4829520]

A single molecule connected to source and drain electrodes through well defined chemical bonds constitutes an ideal system for exploring (coherent) charge and heat flow within a molecule and across a metal-molecule interface.[1,2] Understanding the electronic structure of metal-molecule interfaces, and in particular the energy level alignment and interface conductance, is essential for the development of accurate models in several research fields including organic photovoltaics,[3] (photo-)electrochemical reactions[4,5] and molecular electronics,[6] which all involve charge flow across a metal-molecule interface as a key element.

Molecular transport junctions are also interesting in their own right. A variety of fascinating phenomena, including strong correlation Kondo physics,[7,8] electrostatic gate control,[7,9] magnetic switching,[10,11] and quantum interference,[12–14] have recently been demonstrated at the single-molecule level. However, the most unique property of molecular junctions, which continues to drive new discoveries in the field, is the vast degree of flexibility in the design of molecular components providing atomic-scale handles on the electronic properties.[15–17] The main problem is the lack of atomic-scale control of the metal-molecule interface. Amine anchoring groups have shown promise in some experimental testbeds, offering well defined and reproducible electronic properties.

The effect of chemical modifications of the 1,4-benzenediamine (BDA) molecule on the electrical conductance has been studied experimentally by Venkataraman *et al.*[16] It was shown that the conductance can be tuned, to some extent, by functionalizing the BDA molecule with different side groups. The conductance of BDA is mainly dominated by the highest occupied molecular orbital (HOMO). The HOMO energy level will be shifted up in energy by the introduction of an electron donating (ED) group and down in energy by an electron withdrawing (EW) group. While the effect of different functional groups only lead to relatively small changes in the conductance it still provides an interesting testbed for a theoretical description of the energy level alignment and electronic transport through the molecules. We note in passing that functional side groups can lead to much larger relative conductance changes in molecules showing destructive quantum interference effects, either by tuning or switching on/off the interference effect.[13,14,18]

DFT calculations have previously been performed to investigate the effect of different functional groups on the BDA conductance.[19] Due to the self-interaction error in standard (semi-)local exchange-correlation (xc) functionals, the HOMO level lies too high in energy, and the conductance is typically overestimated by up to several orders of magnitude. This discrepancy has been corrected to some extent by the DFT+Σ method.[19–22] In this method, the positions of the HOMO and LUMO levels are rigidly shifted to correct for the error in the approximate xc functionals. The shift corrects the energy levels for the free molecule in the gas-phase, for which accurate numbers are available, and includes an image charge correction to account for the screening by the electrodes. The

a)Electronic mail: thygesen@fysik.dtu.dk

latter is estimated using a classical electrostatic model, which depends on the positions of two image planes as adjustable parameters. Self-interaction errors and image charge screening could, in principle, also affect the shape of molecular orbitals which thus influence the metal-molecule coupling strength and the broadening of molecular resonances.[23] More recently, the self-consistent GW method has been successfully applied to calculate the conductance of several small molecules.[24–26] It has been demonstrated that the GW scheme, without adjustable parameters, provides quantitative agreement with the experiments for both conductance[25,26] and thermopower.[27]

In this paper, we address the effect of functional groups on the conductance of gold/BDA junctions using the non-equilibrium Green's function method (NEGF) with different levels of theory to describe exchange-correlation (xc) effects. The DFT+Σ method improves on DFT-PBE and yields conductances within a factor 2 of the experimental results for certain positions of the image planes. However, both DFT-PBE and DFT+Σ fail to capture the trends in the conductance observed in experiment and expected from the electron donating or withdrawing character of the functional group. Hartree-Fock (HF) underestimates the conductance by a factor of 20 and also fails to capture the conductance trends. We find that only the GW method predicts both the trend, that is, the relative ordering of conductance amongst the BDA functionalized molecules, as well as the overall magnitude of the conductance in good agreement with experiments.

All the calculations are performed with the GPAW code[28] using the projector-augmented wave method and a numerical atomic orbitals basis set.[29] We use a double zeta with polarization (DZP) basis for Au and a double zeta (DZ) basis for the molecules. We use rather diffuse basis functions for Au corresponding to an energy shift of 0.01 eV. This is essential to obtain a good description of the surface dipole, which is important for a correct alignment of molecular energy levels. With the present basis set, we obtain a work function of 5.4 eV for the flat Au(111) surface in good agreement with the experimental value of 5.31 eV.[30] The molecules are sandwiched between two four-atom Au tips attached to Au(111) surface as illustrated in Fig. 1(a). The supercell contains eight 4×4 Au(111) atomic layers. The geometries of the molecular junctions are optimised by relaxing the molecule and four atom tips until the residual force on any atom is less than 0.01 eV/Å. For the relaxation, we use the PBE[31] functional and a $4 \times 4 \times 1$ k-point sampling. The HF and GW transport calculations are performed according to the method described in Ref. 24. The transmission is calculated from the Landauer formula[32,33]

$$T(\varepsilon) = \mathrm{Tr}[G^r(\varepsilon)\Gamma_L(\varepsilon)G^a(\varepsilon)\Gamma_R(\varepsilon)], \quad (1)$$

where the retarded Green's function is obtained from

$$G^r(E) = [(E + i\eta)S - H_0 + V_{xc} - \Delta V_H[G] - \Sigma_L^r(E) - \Sigma_R^r(E) - \Sigma_{xc}[G](E)]^{-1}. \quad (2)$$

Here S, H_0, and V_{xc} are the overlap matrix, Kohn-Sham (KS) Hamiltonian matrix and the PBE xc-potential in the atomic orbital basis, respectively. η is a numerical positive infinitesimal which is set to 0.02 eV in all the calculations. $\Sigma_{L/R}^r$ are

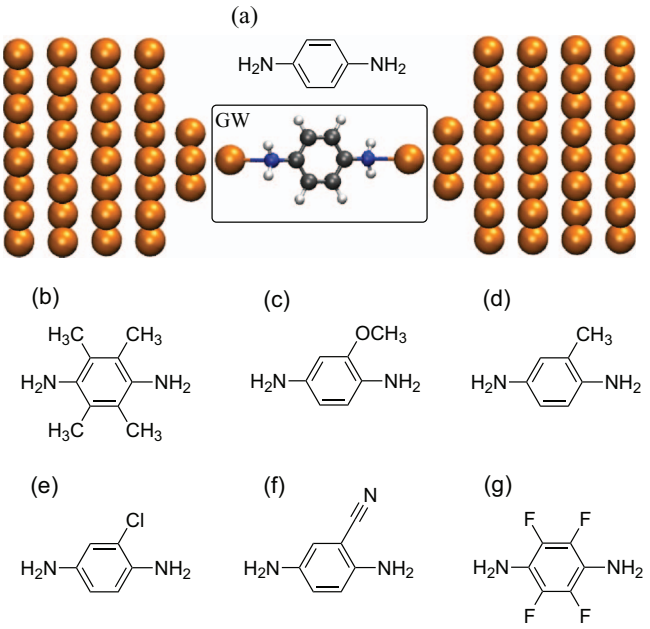

FIG. 1. (a) The atomic structure of the gold/BDA junction. The amine linkers connect the benzene ring to the gold electrodes via two 3-fold coordinated gold atoms. The black box indicates the region where the GW self-energy is evaluated self-consistently. The other structures considered are constructed by replacing BDA by (b) BDA+CH_3*4, (c) BDA+OCH_3, (d) BDA+OCH_3, (e) BDA+Cl, (f) BDA+CN, (g) BDA+F*4.

the retarded lead self-energies and ΔV_H is the deviation of the Hartree potential from the equilibrium DFT-PBE value. Σ_{xc} is the many-body xc self-energy. For HF and GW, Σ_{xc} is the non-local Fock exchange potential and the GW self-energy, respectively. These self-energies are evaluated self-consistently for atomic orbitals centered on atoms within the box region in Fig. 1(a). A standard NEGF-DFT calculation is recovered when Σ_{xc} is taken as KS xc-potential, V_{xc}. The self-consistent cycle is performed by a linear mixing of the Green functions. The energy dependent quantities are represented on an energy grid ranging from −160 eV to 160 eV with an energy-grid spacing of 0.01 eV.

In the DFT+Σ method an orbital dependent self-energy term Σ is included to shift the molecular orbital energies.[19–22] The self-energy term Σ has the form $\sum_n \Delta_n |\psi_n\rangle\langle\psi_n|$, where $\Delta_n = \Delta_{occ}$ for all the occupied states and $\Delta_n = \Delta_{unocc}$ for all the unoccupied states. The states $|\psi_n\rangle$ are the molecular orbitals calculated by diagonalizing the molecular part of the DFT Hamiltonian for the junction. The energy shift Δ_{occ} has two contributions: A correction obtained as the difference between the Kohn-Sham HOMO energy and the vertical ionisation potential (IP) of the molecule in the gas-phase. The IP is evaluated from a ΔSCF calculation involving the PBE ground state energies of the neutral and cation species, i.e., $\mathrm{IP} = E(N-1) - E(N)$. This term mainly corrects for self-interaction errors and moves the occupied states down by 2–3 eV. Likewise, Δ_{unocc} corrects the LUMO to fit the electron affinity EA $= E(N) - E(N+1)$ and moves the unoccupied states up in energy. Second, we include a classical image charge correction due to the screening from the metal electrodes of the HOMO and LUMO charge densities. This correction relies on the assumption that screening by the Au electrodes can be described

classically as two flat conductors characterised by two image planes, the positions of which are adjustable parameters. The image planes are placed symmetrically in the junction. We consider three different positions of the image plane relative to the tip gold atom, namely, $z = -1.0, 0.0, +1.0$ Å.

The junction atomic structure and the functionalized BDA molecules investigated are shown in Fig. 1. For all the junctions, we observe very small structural variations at the contact interface due to the side group substitution. The average Au-N bond length is 2.55 Å with standard deviation (STD) of 0.026 Å and the average Au-N-C angle is 130.4° with STD of 3.1°. It is known, both experimentally and theoretically, that the conductance is relatively insensitive to the contact geometry for amine-linked junctions.[20,34] Previous calculations also show that, for the most stable configurations, the conductance remains essentially constant when the Au-N bond length is changed by up to 0.05 Å.[35] Since the STD of the Au-N bond length obtained for the molecules is only 0.026 Å, we conclude that the origin of the conductance variation observed for the functionalized junctions is an electronic rather than a structural effect.

The transmission functions for the unsubstituted BDA junction calculated using DFT-PBE, HF, and GW are shown in Figs. 2(a) and 2(b) shows a zoom of the transmission of all the different functionalized BDA junctions around the Fermi energy on a logarithmic scale. For each method, we find that the functional group only induces small changes in the shape and value of the transmission around the Fermi energy. This indicates that the effect of functional group on conductance is weak, in agreement with the experiment. In all cases, the Fermi level is crossing the tail of a HOMO resonance peak, indicating that the HOMO level is mediating the charge transport. We note that the slope of the transmission function at the Fermi energy is an indicator for the Seebeck coefficient. The negative slope signals HOMO-mediated transport in agreement with measurements of the Seebeck coefficient of gold BDA junctions.[22]

The positions of the HOMO resonance in the junction and in the gas-phase are shown in Figs. 3(a) and 3(b), respectively. In addition, we show the results obtained with the DFT+Σ approach. To define the HOMO level position in the junction we have used the position of the first transmission peak below the Fermi level reaching a value of 0.8–1. The functional groups have been ordered according to their electron donating/withdrawing nature with the most donating groups to the left and most withdrawing groups to the right. The position of the HOMO level is seen to follow this trend both in the junction and the gas-phase.

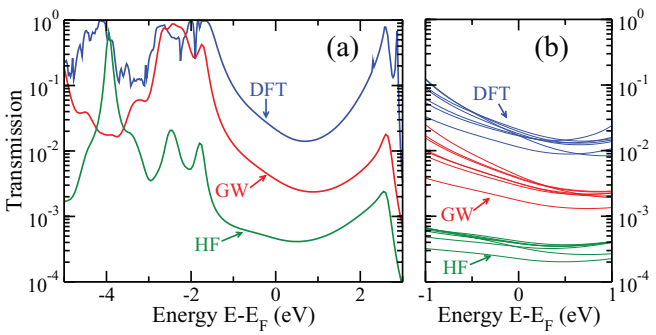

FIG. 2. (a) The transmission function for the unsubstituted BDA junction calculated by DFT-PBE (blue), Hartree-Fock (green), and the self-consistent GW approximation (red). (b) The transmission functions for the different functionalized BDA junctions.

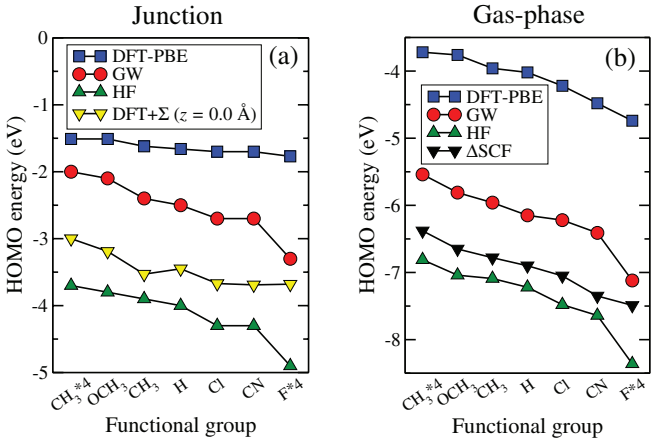

FIG. 3. (a) The HOMO positions relative to the Fermi level of different functionalized BDA junctions calculated by using DFT-PBE (blue), HF (green), the self-consistent GW approximation (red), and DFT+Σ (yellow). The position of the HOMO is taken as the first transmission peak below the Fermi level. (b) HOMO level positions in the gas-phase relative to the vacuum level.

Focusing on the gas-phase, we see that although all methods give the same trend for the HOMO level position, there are considerable differences both in the absolute values as well as the relative differences between the molecules. Taking either GW or ΔSCF as a reference, the DFT-PBE levels are typically overestimated by 2-3 eV while HF underestimates by 0.5–1 eV. The large overestimation of the HOMO level by DFT-PBE can be explained by the spurious self-interaction. In contrast, the self-interaction free HF approximation underestimates the HOMO due to the missing correlation. All methods predict similar trends for the dependence of the HOMO energy on the functional group, except for the F*4 group where DFT+Σ and DFT-PBE predict give much smaller change than HF and GW.

We note that the GW results for the IPs lie around 1 eV above the IPs predicted by the ΔSCF method. For BDA, the IP predicted by GW (6.2 eV) is 1–1.5 eV smaller than the experimental vertical IP which lies in the range 7.3–7.6 eV.[36] Thus, it seems that the gas-phase IPs obtained with GW are on the order 1 eV too small for the present set of molecules. This is somewhat larger than that reported previously by some of us for a test set of 34 small molecules (mean deviation from experiments of 0.4 eV).[37] We ascribe this difference to the different basis sets employed. In Ref. 37 we used a DZP basis set comprising maximally localized Wannier functions constructed from a highly accurate real space grid DFT calculation augmented by numerical atomic orbitals, whereas the present calculations are performed with a DZ basis of numerical atomic orbitals. We further note that previous plane wave G_0W_0 calculations found an IP for BDA of 7.0 eV.[38] This result is more consistent with the mean deviation of 0.4 eV reported in Ref. 37 and indicates that our present basis set is not

TABLE I. Summary of conductances (in units of $10^{-3}G_0$) obtained with DFT-PBE, GW, Hartree-Fock, and DFT+Σ for different image plane positions, namely $z = -1.0$, 0.0, +1.0 Å relative to the Au tip atom. The experimental conductances are listed in the last column.[16]

					DFT+Σ			
	Effect	DFT	GW	HF	− 1.0 Å	0.0 Å	+1.0 Å	Expt.
CH_3*4	donor	17.2	4.15	0.337	4.41	6.24	10.79	8.2 ± 0.2
OCH_3	donor	19.6	3.85	0.385	3.37	4.26	6.23	6.9 ± 0.2
CH_3	donor	18.2	3.76	0.393	3.16	3.77	5.81	6.4 ± 0.6
H		21.3	3.67	0.459	3.57	4.51	6.69	6.4 ± 0.2
Cl	acceptor	17.2	3.19	0.384	3.35	3.88	5.90	6.0 ± 0.4
CN	acceptor	16.7	2.91	0.343	3.05	3.52	5.29	6.0 ± 0.3
F*4	acceptor	11.3	1.74	0.225	3.42	4.13	6.65	5.5 ± 0.3

fully converged for gas-phase calculations. We would like to stress, however, that the accuracy of our GW calculations are expected to be higher for the molecules in the junction than for the gas-phase. This is because in the junction, the screened interaction entering the GW self-energy is dominated by the response function of the gold electrodes. The latter is mainly determined by low-energy transitions ($s - s$ intraband and $s - d$ interband transitions), which are well represented by our DZP basis set. The last point follows from the excellent agreement between the band structure of bulk gold obtained with our DZP basis and a plane wave basis set (not shown). Moreover, it is our experience that standard G_0W_0 quasiparticle calculations for metallic systems converge much faster with respect to plane wave cut-off than calculations for isolated molecules. Based on this we expect our GW calculations for the contacted molecules to be less sensitive to the finite basis set than the gas-phase calculations.

The general trends in the HOMO level position observed in the gas-phase are also seen for the contacted molecules, see Fig. 3(a). The relative HOMO resonance position in the junction with GW and HF is almost unchanged from the gas-phase and still shows a variation of around 1.5 eV. However, with DFT-PBE the HOMO resonance position varies much less with the functional group compared to the gas-phase and shows a total variation of only 0.25 eV. We ascribe this to a stronger pinning of the HOMO to the Fermi level in the DFT-PBE calculations. The stronger pinning results from the larger overlap of the HOMO resonance with the Fermi level in DFT and from the spurious self-interaction which enhances the effective fields making it energetically more difficult for charge to flow to/from the HOMO. Additionally, the DFT+Σ inherits the strong pining in DFT and therefore shows a small total variation of 0.7 eV.

We note that the DFT-PBE levels are in general closer to the GW levels in the junction than in the gas-phase. This is a result of the enhanced screening by the metal electrodes which pushes the HOMO level upwards in energy when the molecule is placed in the junction.[39,40] This effect is completely missed by Hartree-Fock and DFT. However, our GW method naturally captures this feature, which can be seen from the increased distance between the GW and HF levels when going from the gas-phase to the junction in Fig. 3. For the functionalized BDA junctions, the image charge shift amounts to around 0.4 eV on average.

The calculated zero-bias conductances obtained from $G = G_0T(E_F)$, where $G_0 = 2e^2/h$ is the conductance quantum, are shown in Fig. 4. The corresponding values are listed in Table I. We find that DFT-PBE overestimates the experimental conductances by a factor of 3, while HF underestimates the experimental conductances by a factor of 20. Inclusion of screening at the GW level brings the conductances closer to experimental values, but the method still underestimates the experimental values by a factor of 2.

Interestingly, only GW correctly predicts the relative effect of the functional groups. Specifically, functional groups with donor characteristic such as CH_3*4, OCH_3, and CH_3 increase the conductance, while functional groups with acceptor characteristic such as Cl, CN, and F*4 decrease the conductance. Although the variations in conductance are small, they correlate well with the variations in the HOMO positions and with the expected effects of the side groups. In the case of DFT, although the changes of the DFT HOMO positions follow the ED and EW effects of the substituent groups, the conductances do not follow this trend. From Fig. 3, as already mentioned, the changes of the DFT HOMO positions are relatively small compared to the GW results due to the stronger effect of pinning to the metal Fermi level. Consequently, the variation in the DFT conductance is more sensitive to other

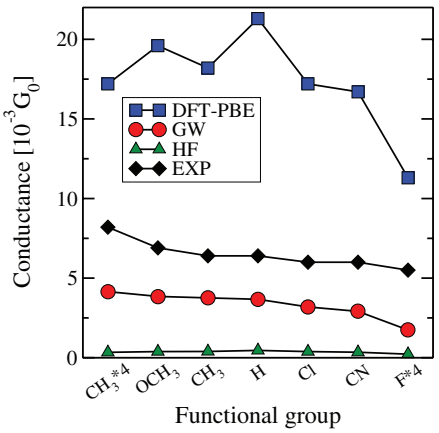

FIG. 4. Conductance of side group functionalized BDA junctions calculated with DFT-PBE (blue), Hartree-Fock (green), and self-consistent GW (red). The experimental conductances are shown in black.

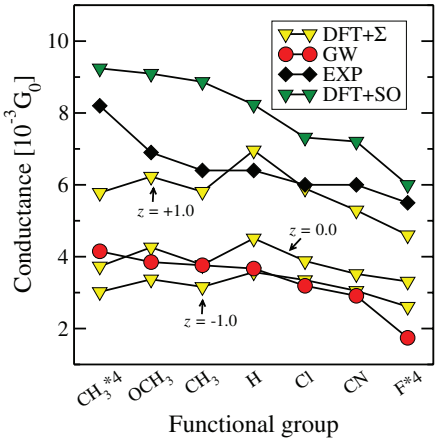

FIG. 5. Conductance of the functionalized BDA junctions calculated using the DFT+Σ method (yellow) with three different image plane positions, namely, $z = -1.0$, 0.0, $+1.0$ Å relative to the Au tip atom, compared with the GW (red), DFT+SO (green), and experimental (black) results. Note in DFT+SO method, the positions of DFT HOMO and LUMO levels are shifted with a scissor operator to match the positions of GW HOMO and LUMO levels.

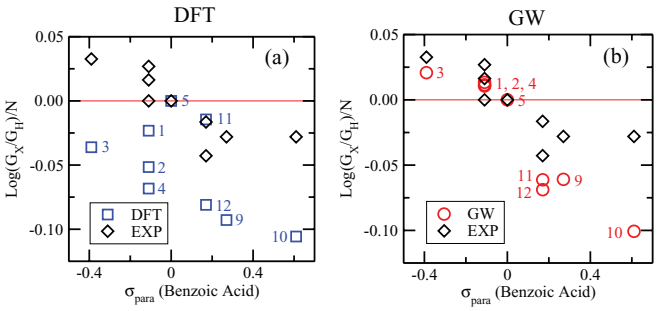

FIG. 6. Logarithm of the ratio of the functionalized molecule conductance (G_X) to the BDA conductance (G_H) divided by the number of side groups (N) in each molecule against the Hammmett σ_{para} coefficient from Ref. 42. (a) DFT calculations. (b) GW calculations. Note that the labels used for the molecules follow Ref. 16 for the ease of comparison.

effects, such as the variation in the coupling strengths, and does not reflect the (small) variation in the level positions.

In Fig. 5, we compare the DFT+Σ results with GW and experimental values. The conductances of the $z = +1.0$ Å image plane position gives results in overall best agreement with the experimental values. Shifting the image planes further away from the molecule by $z = -1.0$ Å or $z = 0.0$ Å reduces the image charge energies. This implies that the molecular levels are shifted away from the Fermi level, and the conductances are lowered to values closer to the GW results. While the DFT+Σ results are in overall good agreement with the experiments, the changes in conductance with different side groups are not correctly captured by this method. Interestingly, if the positions of the DFT HOMO and LUMO levels are shifted using a scissor operator (DFT+SO) to match the positions of GW HOMO and LUMO levels, the correct ordering of the conductance is recovered. We note in passing that the relative conductance difference between the DFT+SO and GW is related to the frequency dependence of the GW self-energy which is absent in DFT+SO.[41] The DFT+SO results further support the interpretation that the wrong ordering of the conductances in DFT and DFT+Σ is a consequence of incorrect level alignment.

In their original work Venkataraman *et al.* explored the connection between the change induced by a side group on the tunnel conductance and reaction rate of the BDA, respectively.[16] To this end, they plotted the log of the ratio of the measured conductance for the substituted (G_X) and unsubstituted (G_H) molecule scaled by the number of substituents on the ring against the Hammett parameter σ_{para}. In Fig. 6 we have made a similar plot comparing our calculated data with the measured data from Ref. 16 and taking Hammett constants from Ref. 42. Overall, there is a good agreement between the GW and experimental data sets. In particular, the clear trend that the conductance decreases as the Hammett constant is made more positive is well reproduced by GW. In contrast the DFT results do not show this trend. The non-additive dependence on the number of substituent groups (labels 1,2,4 for methyl and 11,12 for fluorine) is, however, not well accounted for by GW which underestimates the change in conductance with the number of groups compared with experiments.

The results presented above demonstrate a quantitative agreement between experiments and self-consistent GW transport calculations. Although the GW conductances are still around a factor of two lower than the experiments, the agreement is indeed satisfactory given the statistical variations in the metal-molecule linker structure, solvent, and temperature effects. In a recent study we have investigated the influence of structural effects on the BDA conductance.[27] At the level of DFT+Σ we found that the conductance varied by about a factor of two for different junction geometries in agreement with previous work,[20] and similar structure-induced variation are expected at the GW level. In contrast to the DFT-based calculations, the variations in GW conductance for different side groups follow the experimental trends as well as the variations in the HOMO position as expected from the donating/accepting character of the functional groups.

We have found that the DFT+Σ method gives conductance values in close agreement with experiment for image plane positions at $z = +1.0$ Å. On the other hand, the closer agreement with the more accurate GW calculations for $z = 0.0$ Å or $z = -1.0$ Å might just as well suggest that these are more correct positions of the image planes. More importantly, both DFT and DFT+Σ show, irrespective of image plane positions, a very similar relative ordering of the conductance, although the absolute position of the frontier energy levels are rather different in the two methods. This is a consequence of the strong pinning of the DFT molecular resonances to the metal Fermi level an effect which is inherited by the DFT+Σ method.

In conclusion, we have explored the role of energy level alignment for a correct description of the electronic conductance of side group functionalized benzene-diamine molecular junctions. The self-consistent GW method was found to yield excellent agreement with experiments for both qualitative trends and absolute conductance values. In contrast, standard DFT as well as the scissors operator corrected DFT+Σ method failed to reproduce the relative variation in

conductance with functional group. This result could be explained by incorrect energy level alignment predicted by DFT due to over-pinning of the molecular levels to the metal Fermi level.

ACKNOWLEDGMENTS

T.M. acknowledges support from the Danish Council for Independent Research, FTP Grant Nos. 11-104592 and 11-120938. K.S.T. and C.J. acknowledge support from the Danish Council for Independent Research, FTP Sapere Aude Grant No. 11-1051390. G.C.S. and M.S. received funding from the European Research Council under the European Union's Seventh Framework Programme (FP7/2007-2013)/ ERC Grant agreement No. 258806.

[1]C. Joachim, J. K. Gimzewski, and A. Aviram, Nature (London) **408**, 541 (2000).
[2]Y. Dubi and M. DiVentra, Rev. Mod. Phys. **83**, 131 (2011).
[3]J.-L. Brdas, J. E. Norton, J. Cornil, and V. Coropceanu, Acc. Chem. Res. **42**, 1691 (2009).
[4]I. E. Castelli, D. D. Landis, K. S. Thygesen, S. Dahl, I. Chorkendorff, T. F. Jaramillo, and K. W. Jacobsen, Energy Environ. Sci. **5**, 9034 (2012).
[5]I. E. Castelli, T. Olsen, S. Datta, D. D. Landis, S. Dahl, K. S. Thygesen, and K. W. Jacobsen, Energy Environ. Sci. **5**, 5814 (2012).
[6]K. Moth-Poulsen and T. Bjornholm, Nat. Nanotechnol. **4**, 551 (2009).
[7]S. Kubatkin, A. Danilov, M. Hjort, J. Cornil, J.-L. Bredas, N. Stuhr-Hansen, P. Hedegard, and T. Bjornholm, Nature (London) **425**, 698 (2003).
[8]W. Liang, M. P. Shores, M. Bockrath, J. R. Long, and H. Park, Nature (London) **417**, 725 (2002).
[9]H. Song, Y. Kim, Y. H. Jang, H. Jeong, M. A. Reed, and T. Lee, Nature (London) **462**, 1039 (2009).
[10]S. Sanvito, Chem. Soc. Rev. **40**, 3336 (2011).
[11]M. Diefenbach and K. Kim, Angew. Chem., Int. Ed. **46**, 7640 (2007).
[12]P. Sautet and C. Joachim, Chem. Phys. Lett. **153**, 511 (1988).
[13]D. Q. Andrews, G. C. Solomon, R. P. Van Duyne, and M. A. Ratner, J. Am. Chem. Soc. **130**, 17309 (2008).
[14]C. M. Guedon, H. Valkenier, T. Markussen, K. S. Thygesen, J. C. Hummelen, and S. J. van der Molen, Nat. Nanotechnol. **7**, 305 (2012).
[15]L. Venkataraman, C. Nuckolls, M. S. Hybertsen, and M. L. Steigerwald, Nature (London) **442**, 904 (2006).
[16]L. Venkataraman, Y. S. Park, A. C. Whalley, C. Nuckolls, M. S. Hybertsen, and M. L. Steigerwald, Nano Lett. **7**, 502 (2007).
[17]A. Mishchenko, D. Vonlanthen, V. Meded, M. Brkle, C. Li, I. V. Pobelov, A. Bagrets, J. K. Viljas, F. Pauly, F. Evers *et al.*, Nano Lett. **10**, 156 (2010).
[18]T. Markussen, R. Stadler, and K. S. Thygesen, Nano Lett. **10**, 4260 (2010).
[19]D. J. Mowbray, G. Jones, and K. S. Thygesen, J. Chem. Phys. **128**, 111103 (2008).
[20]S. Y. Quek, L. Venkataraman, H. J. Choi, S. G. Louie, M. S. Hybertsen, and J. B. Neaton, Nano Lett. **7**, 3477 (2007).
[21]S. Y. Quek, H. J. Choi, S. G. Louie, and J. B. Neaton, Nano Lett. **9**, 3949 (2009).
[22]S. Y. Quek, H. J. Choi, S. G. Louie, and J. B. Neaton, ACS Nano **5**, 551 (2011).
[23]M. Strange and K. S. Thygesen, Phys. Rev. B **86**, 195121 (2012).
[24]K. S. Thygesen and A. Rubio, Phys. Rev. B **77**, 115333 (2008).
[25]M. Strange, C. Rostgaard, H. Häkkinen, and K. S. Thygesen, Phys. Rev. B **83**, 115108 (2011).
[26]M. Strange and K. S. Thygesen, Beilstein J. Nanotechnol. **2**, 746 (2011).
[27]T. Markussen, C. Jin, and K. S. Thygesen, "Quantitatively accurate calculations of conductance and thermopower of molecular junctions," Phys. Status Solidi B (published online).
[28]J. Enkovaara, C. Rostgaard, J. J. Mortensen, J. Chen, M. Dułak, L. Ferrighi, J. Gavnholt, C. Glinsvad, V. Haikola, H. A. Hansen *et al.*, J. Phys.: Condens. Matter **22**, 253202 (2010).
[29]A. H. Larsen, M. Vanin, J. J. Mortensen, K. S. Thygesen, and K. W. Jacobsen, Phys. Rev. B **80**, 195112 (2009).
[30]H. B. Michaelson, J. Appl. Phys. **48**, 4729 (1977).
[31]J. P. Perdew, K. Burke, and M. Ernzerhof, Phys. Rev. Lett. **77**, 3865 (1996).
[32]Y. Meir and N. S. Wingreen, Phys. Rev. Lett. **68**, 2512 (1992).
[33]K. S. Thygesen, Phys. Rev. B **73**, 035309 (2006).
[34]L. Venkataraman, J. E. Klare, I. W. Tam, C. Nuckolls, M. S. Hybertsen, and M. L. Steigerwald, Nano Lett. **6**, 458 (2006).
[35]M. S. Hybertsen, L. Venkataraman, J. E. Klare, A. C. Whalley, M. L. Steigerwald, and C. Nuckolls, J. Phys.: Condens. Matter **20**, 374115 (2008).
[36]See http://webbook.nist.gov/cgi/cbook.cgi?ID=C106503&Units=SI&Mask=20#Ion-Energetics for gas phase ion energetics data (accessed 13 June 2013).
[37]C. Rostgaard, K. W. Jacobsen, and K. S. Thygesen, Phys. Rev. B **81**, 085103 (2010).
[38]I. Tamblyn, P. Darancet, S. Y. Quek, S. A. Bonev, and J. B. Neaton, Phys. Rev. B **84**, 201402 (2011).
[39]J. B. Neaton, M. S. Hybertsen, and S. G. Louie, Phys. Rev. Lett. **97**, 216405 (2006).
[40]J. M. Garcia-Lastra, C. Rostgaard, A. Rubio, and K. S. Thygesen, Phys. Rev. B **80**, 245427 (2009).
[41]C. J. Jin and K. S. Thygesen, "Dynamical image charge effect in electron tunneling beyond energy level alignment," e-print arXiv:1311.0163v1 (unpublished).
[42]C. Hansch, A. Leo, and R. W. Taft, Chem. Rev. **91**, 165 (1991).